

# Effective and recovery stresses in deformation studies of polyvinyl chloride and polypropylene using the modified strain transient dip test

S. H. TEOH, A. N. POO, G. B. ONG

*Department of Mechanical and Production Engineering, National University of Singapore, 10 Kent Ridge Crescent, Singapore 0511*

Partitioning the applied stress into internal stress components (effective and recovery) using the modified strain transient dip test is a useful approach towards a better understanding of the viscoelastic nature of polymers. The internal stresses of polyvinyl chloride (PVC) and polypropylene (PP) were measured successfully using this test on a computer-controlled electro-servo hydraulic tensile testing machine which was designed for rapid step unloading in less than 1 s to avoid memory effects of the polymers. A power-law relationship can be used to describe the variation of the internal stress components with strain. Actual yield strains occurred at smaller values (less than 2%) than those obtained from a conventional stress-strain diagram (which for PVC and PP exceed 3.5% and 7%, respectively). This observation indicated that plastic yielding occurred much earlier and yield strains from conventional stress-strain diagrams may be overestimates. For very ductile material (PP) the activation volumes were comparable in magnitude to that obtained conventionally; whilst for less ductile material (PVC), the activation volume was four times higher. One of the main advantages of stress partitioning is for the detailed definition of the extrapolated yield point which otherwise will be missed out in a conventional plot of applied stress and strain.

## 1. Introduction

The main objective of internal stress measurements through applied stress partitioning is to enable proper and more accurate mathematical, as well as physical, modelling of polymers. Such a study may also allow identification of the components that are responsible for failure. The mechanical behaviour of polymers is traditionally characterized by using stress-strain diagrams obtained from conventional universal tensile testing machines. This has been a long established field. However, detailed knowledge in terms of the role of the internal stresses that can be obtained from these conventional methods, is limited.

The measurement of internal stresses in terms of partitioning the applied stress,  $\sigma_{ap}$ , into the effective,  $\sigma_{ef}$ , and the recovery,  $\sigma_{re}$ , stress (the former is related to the viscous flow while the latter is related to the recovery component of the polymer) is a necessary step towards a better understanding of the viscoelastic properties of polymers. Mathematically, partitioning the applied stress into internal stress components can be written as

$$\sigma_{ap} = \sigma_{ef} + \sigma_{re} \quad (1)$$

This expression can best be visualized by a three-element model as shown in Fig. 1a. The model has two linear springs. One of these is paralleled by a non-linear (Eyring) rate-activated dashpot element and is characterized by a modulus  $E_a$  which in this paper,

because it represents the elastic component of the anelastic (time dependent) deformation, is termed the anelastic modulus. The second spring is characterized by a modulus  $E_e$  which, because it represents the instantaneously elastic deformation of the polymer, is termed the elastic modulus. The moduli of these springs can be thought of as representing the deformation of molecular domains (Fig. 1b) in chain segment direction,  $E_e$ , and perpendicular to it,  $E_a$ , and can be physically related to the stretching of the C-C bond and the van der Waals forces acting between chains, respectively [1]. Such a model helps one to have a physical picture of the deformation process in polymers associated with stress partitioning and will be useful when interpreting experimental results.

At present we are unaware of any other computer-aided testing equipment which is capable of performing the above transient test which requires rapid loading and unloading, typically in less than a few seconds. Although Teoh and co-workers [2, 3] has adopted a modified strain transient dip test for both creep and constant strain-rate conditions on an old Instron Universal tester, the challenge remains in stress partitioning experiments through proper computer-aided equipment design. The modified strain transient dip test follows that of the alternate creep-creep-recovery method which was reviewed and discussed in a previous publication [3]. It must be noted that significant work has been done on creep-

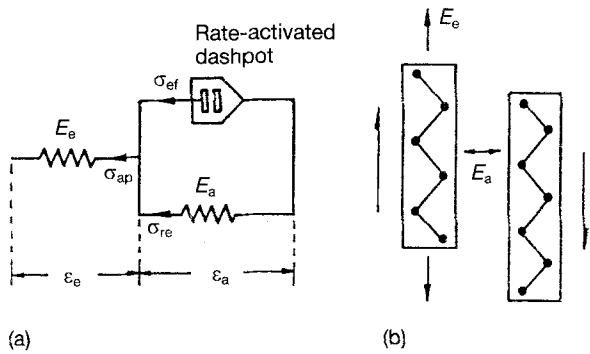


Figure 1 (a) Three-element model showing the partitioning of the applied stress into recovery and effective stresses. (b) Molecular representation of the three-element model [1].

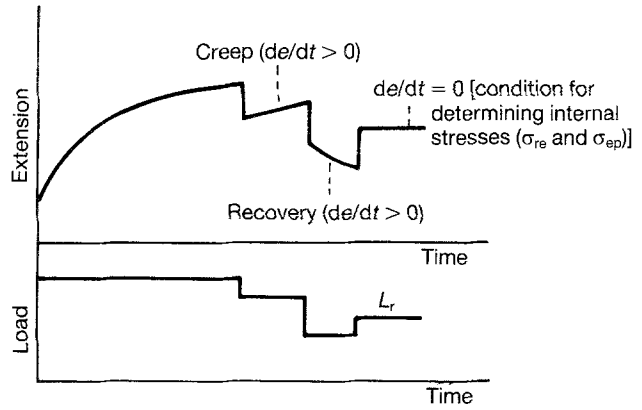


Figure 2 The alternate creep-creep-recovery method of measuring internal stresses of materials.

recovery experiments of polymers and just samples of the many reported work are cited [4–6].

This paper reports on two polymers, polyvinyl chloride (PVC) and polypropylene (PP), that were tested using the modified strain transient dip tests which was designed to carry out the stress partitioning for deformation under constant load (creep) and strain-rate conditions in an electro-servo-hydraulic tensile tester. The development and fabrication of this specialized electro-servo-hydraulic tensile testing machine is also highlighted. Rapid unloading of less than 1 s was designed to take into account the memory effect of the polymers.

### 1.1. Strain transient dip test

Alquist and Nix [7] were among the earliest researchers to use the alternate creep-creep-recovery method for the strain transient dip test. This test was also carried out by Bergman [8]. Basically, this method relies on the load reductions made during a creep experiment. The constant load applied to the specimen is interrupted by a small reduction load. Immediately after a load reduction, a rapid contraction (elastic response) is observed and, depending upon the magnitude of the reduction, the immediate extension rate ( $de/dt$ ) can either be positive, negative or zero. The load that remains on the specimen, after a load reduction that produces the zero extension rate condition ( $L_r$  in Fig. 2), is then taken to be the recovery stress. The creep indicated by a positive extension rate is thought of as being controlled by the effective stress.

An understanding of the above responses to load reduction can be made by rewriting Equation 1 as

$$\sigma_{ef} = \sigma'_{ap} - \sigma_{re} \quad (2)$$

where  $\sigma'_{ap}$  is the stress immediately after load reduction.

$$\text{If } \sigma'_{ap} > \sigma_{re}, \text{ then from Equation 2} \\ \sigma_{ef} > 0; de/dt > 0 \text{ (creep)} \quad (3)$$

$$\text{If } \sigma'_{ap} < \sigma_{re}, \text{ then} \\ \sigma_{ef} < 0; de/dt < 0 \text{ (recovery)} \quad (4)$$

$$\text{However, if } \sigma'_{ap} = \sigma_{re}, \\ \sigma_{ef} = 0; de/dt = 0 \quad (5)$$

As written, Equation 5 enables the recovery stress to

be measured. The load that produces this zero extension rate condition gives the recovery stress. From Equation 1, knowing  $\sigma_{ap}$  and  $\sigma_{re}$ ,  $\sigma_{ef}$ , can then be determined. However, the time frame for the above method is too long and not suitable for polymers and must be modified.

The modified strain transient dip test by Teoh *et al.* [3] involved rapid step unloading (time scale of the measurement was more than 1 s per step unloading) and extrapolating to zero extension rate (Fig. 3) on a single specimen. The technique can be applied to polymers under uniaxial creep or constant strain-rate

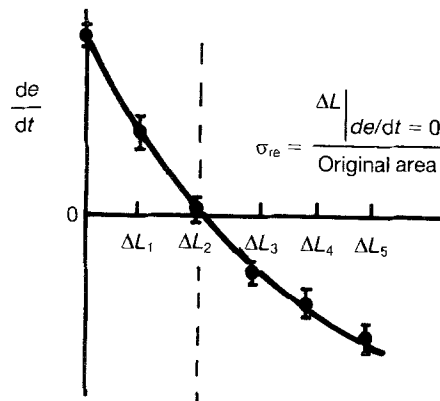
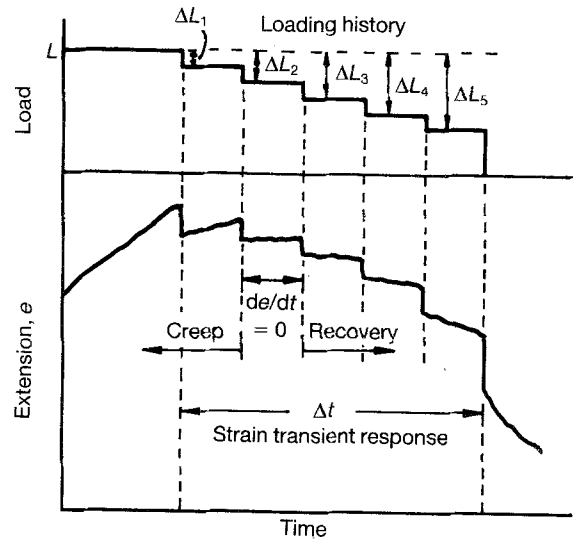


Figure 3 (a) Schematic drawing of the modified strain transient dip test [3]. (b) Plot of load reduction against  $de/dt$  [3].

conditions. The strain response after unloading is always dependent on the history of previous imposed loads due to memory effects arising from the viscoelastic nature of polymers [4-6]. The interpretation of results, therefore, may only be valid for a particular set of experiments.

### 1.2. Mechanical testing equipment.

Mechanical testing is one of the most fundamental methods for evaluating the performance of materials in service, design and quality control. Material testing systems include those for evaluation of materials performance of metals, composites, ceramics, plastics and rubbers. Many types of machines for mechanical testing of rubbers and plastics have appeared in the market in recent years. Recent trade exhibitions, conferences, reviews and write-ups have indicated that this field is highly competitive and undergoing rapid change. This rapid development is further accelerated by the application of microprocessors not only in data collection but also in complex electronic control of the driving mechanisms using highly efficient ball screws to close-looped servo hydraulic type. Many companies in USA, UK, Europe, and Japan, such as Instron, Shenck, MTS, and Shimadzu, have incorporated microcomputer control in almost all their models. The range of machines produced vary from static to dynamic testing systems either in table top (horizontal or vertical) model or floor standing type. The problem with these commercial products is that the hardware and software supplied by the manufacturer are usually not versatile enough for specialized applications. In many cases, redevelopment and reprogramming of the entire control are needed. For these reasons, it is considered advantageous to pur-

chase only the hardware needed and to develop all the controls and testing software oneself in order to make the system meet special requirements.

In the field of mechanical testing of rubbers and plastics, equipment design is different from those for metals or ceramics. This is because the majority of these materials undergo large deformation, with low modulus, high recovery stress and show significant viscoelasticity with significant memory effects. Therefore, design of the loading frame, gripping device, drive mechanisms and the control strategies have to be looked into with respect to the viscoelastic nature of the material.

## 2. Experimental procedure

The computer-controlled electro-hydraulic servo testing system [9] developed consists of a closed-loop electro-hydraulic servo actuator interfaced with a microcomputer. The basic unit is built up of the following six elements, namely the stiff four-column load frame, the electro-hydraulic servo-drive mechanism, the hydraulic gripping device, the load and displacement sensors, the control and the data acquisition system. A schematic view of the system is shown in Fig. 4.

The materials studied were polyvinyl chloride (PVC) and polypropylene (PP). The PVC came in rigid glass-clear pressed sheets of thickness 2 mm and designated "Sunloid A-100" by the supplier (Tsutsunaka Plastic Industry, Japan). The PP came in rigid white pressed sheets of thickness 3 mm and designated "Trovidus 500 (stress relieved)" by the supplier (Dynamit Nobel Ames, USA). Dumb-bell test specimens conforming to ASTM D638 Type IV were cut from the PVC and PP sheets using a polymer router which

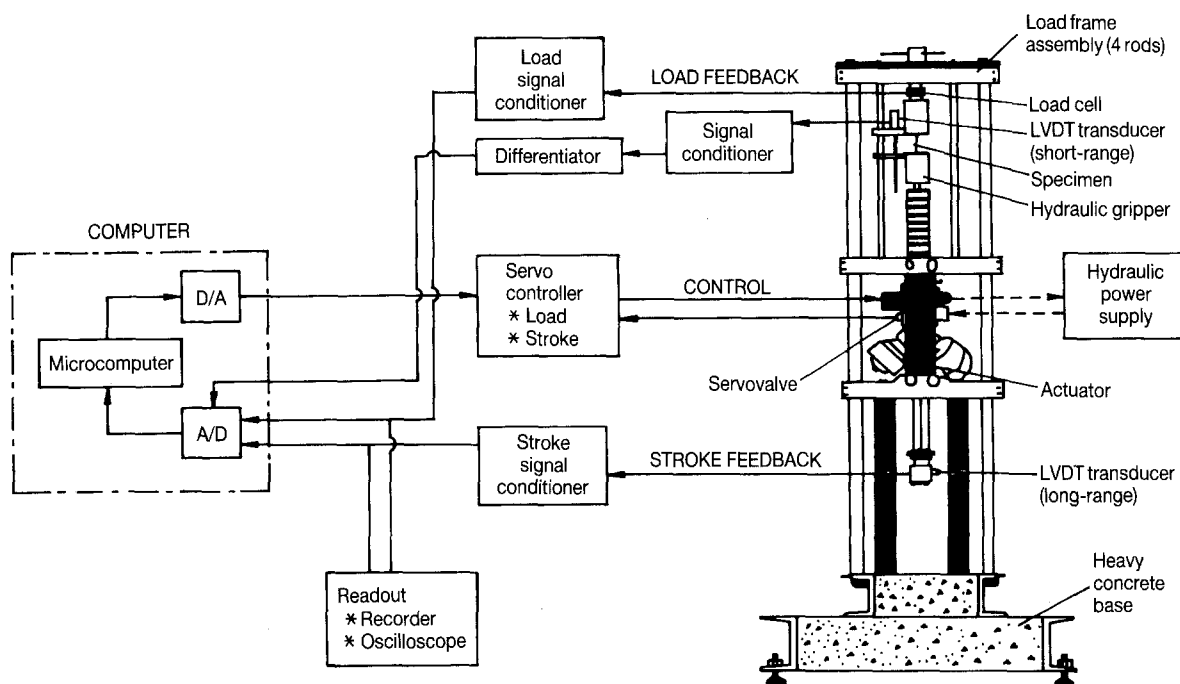


Figure 4 Closed-loop computer-controlled electro-hydraulic servo material testing system designed for the modified strain transient dip testing of polymers.

had a cutting speed of 2400 r.p.m. This high cutting speed was chosen because it gave a consistent and clean surface finish.

The strain transient dip tests were carried out at nine cross-head speeds (CHS) ranging from 0.05–20.00  $\text{cm min}^{-1}$  for PVC and seven cross-head speeds ranging from 0.2–20.00  $\text{cm min}^{-1}$  for PP materials. One specimen was used for each series of load reductions, because structural elements that give rise to the recovery stress may themselves relax. If more than one series of load reductions was performed on the same specimen, at different applied loads, the variation of recovery stress may not be representative for the particular strain rate or applied strain. For each cross-head speed, the recovery stresses for six applied stresses prior to yielding were determined. The tests were carried out at strains below the nominal yield strain as the deformation below the nominal yield point is not complicated by necking and general yielding. Typical results for the strain transient dip test showing the extension response to load reduction are shown in Fig. 5.

By plotting the load reduction against the extension rate (Fig. 3b), the load at which zero extension rate ( $de/dt$ ) occurred was determined. Fig. 6 shows the typical response of extension rate (output from the differentiator) immediately after each load reduction step and Fig. 7 shows the corresponding plot of load reduction against extension rate.

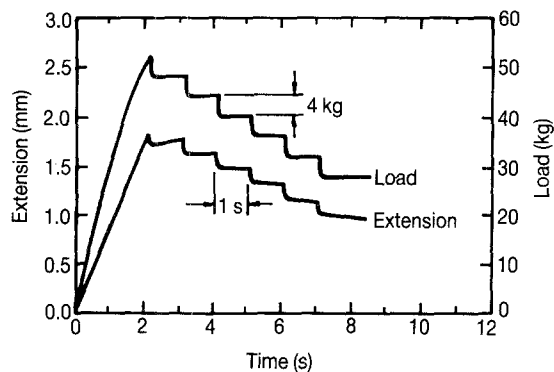


Figure 5 Typical results of the extension response to load reduction, for PP ( $5 \text{ cm min}^{-1}$ ).

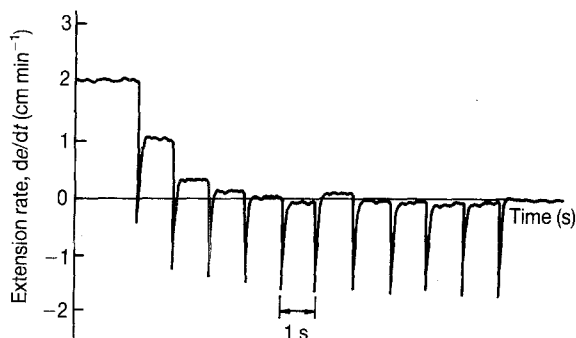


Figure 6 Response of immediate extension rate  $de/dt$  to load reduction steps for a PP specimen unloaded from a maximum applied stress of 23 MPa and a crosshead speed of  $2 \text{ cm min}^{-1}$ .

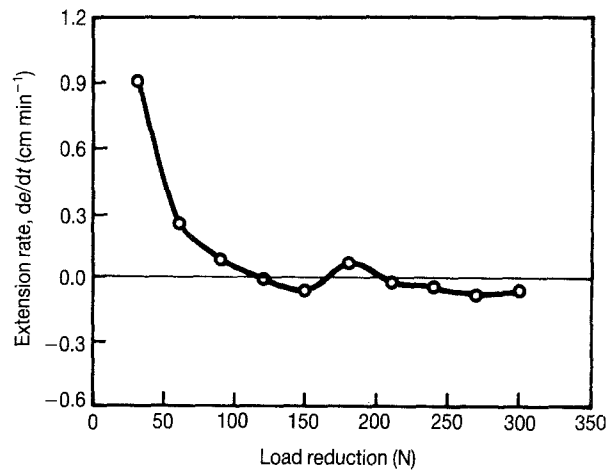


Figure 7 A plot of load reduction against extension rate,  $de/dt$ , for a PP specimen unloaded from a maximum applied stress of 23 MPa and a crosshead speed of  $2 \text{ cm min}^{-1}$ .

It can be noted that the immediate extension rate response is quite consistent for the first five load reduction steps. After 5 s (five steps), the memory effect comes in. Therefore, only the first five extension rates were used to determine the load reduction at zero extension rate. The intercept at which  $de/dt$  is zero was taken to be the effective load. The effective stress was obtained from the ratio of the effective load and the original cross-sectional area of the specimen. The recovery stress was determined by subtracting the effective stress from the applied stress (ratio of the applied load and original area). The applied strain was obtained by dividing the total extension at the applied load by an effective gauge length of 70 mm. This effective gauge length was determined from a knowledge of the geometry of the specimen [10]. Although, this method of determining the effective gauge length may not be the most accurate method, as a first approximation it is good enough for the present study. All tests were performed at  $23 \pm 1^\circ\text{C}$  and  $65 \pm 5\%$  relative humidity.

### 3. Results and discussion

#### 3.1. Variation of yield stress and yield strain with speed of testing.

The purpose of determining the yield stress and yield strain before the commencement of the strain transient dip tests was to ensure that the stress partitioning experiments were all carried out prior to yielding so that the stress and strain measurements would not be deterred by yielding phenomena such as necking and cold-drawing. The variations of yield stress and yield strain with  $\ln$  crosshead speed, ( $\ln$  CHS) for PVC and PP are shown in Fig. 8a and b, respectively. A linear relationship between yield stress,  $\sigma_y$  (MPa), and  $\ln$  CHS ( $\text{cm min}^{-1}$ ) is observed for PVC and PP. Using linear regression, they can be expressed as

$$\sigma_y(\text{PVC}) = 58.89 + 0.573 \ln \text{CHS} \quad (6)$$

$$\sigma_y(\text{PP}) = 24.49 + 1.971 \ln \text{CHS} \quad (7)$$

Similarly, a linear relationship can be seen for yield

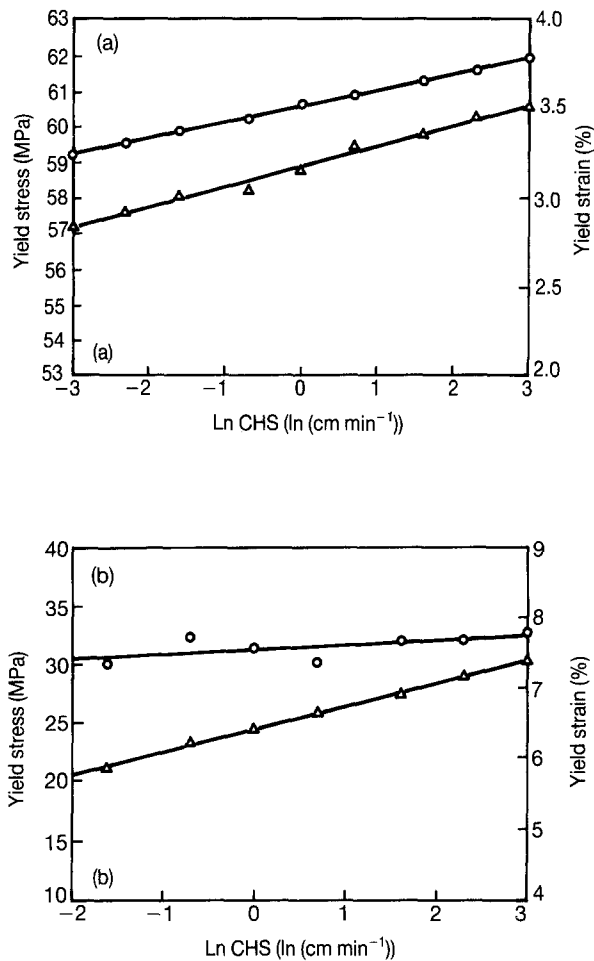


Figure 8 Variation of ( $\Delta$ ) yield stress and ( $\circ$ ) yield strain with ln CHS for (a) PVC and (b) PP.

strain (%) and ln CHS

$$\varepsilon_y(\text{PVC}) = 3.5 + 0.09 \ln \text{CHS} \quad (8)$$

$$\varepsilon_y(\text{PP}) = 7.6 + 0.06 \ln \text{CHS} \quad (9)$$

Generally, from the very small coefficients of ln CHS, it can be noted that the yield strain does not vary significantly with speed of testing and is practically a constant (3.5% and 7.6% for PVC and PP, respectively). These gave an upper strain limit to all the strain transient dip tests.

### 3.2. Pre-fracture phenomena

Pre-fracture phenomena are useful indications of which mechanisms may contribute to ultimate failure [11]. Various pre-fracture phenomena were recorded during the above tests so that results obtained could be correlated. Generally, the PVC specimens tested at CHS greater than 1 cm min<sup>-1</sup> exhibited localized shear bands followed by necking and then fracture. No cold drawing was observed and stress whitening was localized at the neck region. For CHS less than 1 cm min<sup>-1</sup>, the specimens exhibited shear bands, necking, followed by cold drawing before fracture; stress whitening occurred uniformly along the gauge length of the specimen before cold drawing. For the PP specimens, all the specimens tested showed extensive stress whitening along the gauge length followed

by necking and cold drawing. The range of speed tested did not seem to change the occurrence of the pre-fracture phenomena.

### 3.3. Variation of recovery stress with applied strain

Fig. 9a shows the plot of the three stresses (applied, recovery and effective) against applied strain for PVC and Fig. 9b shows that for PP. An obvious result is that as the crosshead speed increases, the maximum value of the effective stress increases while the recovery stress decreases. As has been observed previously [3] the recovery stress deviates further from the applied stress as the speed of testing increases.

From Fig. 9a it can be noticed that, for the case for PVC, the variation of recovery stress with applied strain above a crosshead speed of 0.5 cm min<sup>-1</sup> can almost be represented by a linear relationship described mathematically by

$$\sigma_{re} = A\varepsilon_T \quad (10)$$

where  $A$  is a constant and  $\varepsilon_T$  is the applied strain.

Those at crosshead speed less than 0.5 cm min<sup>-1</sup> appear to have a power-law relationship of the type

$$\sigma_{re} = A\varepsilon_T^n \quad (11)$$

where  $A$  and  $n$  are constant.

For the case of PP (Fig. 9b), it appeared that the recovery stress varies according to Equation 11 for all crosshead speeds. Assuming that the mathematical relationship between the recovery stress and the applied strain can generally be described by Equation 11 (that is, the anelastic spring in Fig. 1a is of a power-law type) one can then investigate the variation of  $A$  and  $n$  with ln CHS. This is shown in Fig. 10 which is an interesting plot. It shows that the  $A$  values for PVC are higher than those of PP and decrease with CHS to an asymptotic value of about 15 MPa, at high CHS. For PP,  $A$  is almost independent of CHS and the average constant value is 6.65 MPa. The variation of  $n$  with CHS at low CHS (less than 0.5 cm min<sup>-1</sup>) seems to be the same in terms of magnitude (about 0.67) for both PVC and PP. At higher CHS,  $n$  for PVC jumps to about 0.93, whereas  $n$  for PP remains the same. For PVC this transition occurs when CHS = 0.6 cm min<sup>-1</sup>. It may appear highly coincidental that for PVC there is a change in pre-fracture phenomena from one without cold drawing to one with cold drawing before fracture at CHS = 1 cm min<sup>-1</sup> which is close to 0.6 cm min<sup>-1</sup>. The same  $n$  value for PP and PVC (at lower CHS) further reinforced the idea that  $n$  is perhaps a significant ductility parameter for polymers. It appeared that if  $n$  is greater than 0.67, cold-drawing will not occur. (It will be interesting to find out whether other polymers have similar results.)

### 3.4. Variation of effective stress with applied strain

The variation of the effective stress with applied strain can best be studied if one refers to the three-element

model in Fig. 1a. One expects some yielding phenomena to be observed on a plot of effective stress and applied strain because some rate-activated process was assumed to be operative in this regime. The yield point is difficult to define when one looks closely at the applied stress against applied strain in Fig. 9a and b. In order to study this further, a plot of effective stress against strain was made and this is shown in Fig. 11a and b for PVC and PP, respectively. It can be seen that the effective stress approaches an asymptotic value for each CHS. From these figures, one can define the extrapolated yield point (EYP) [3] quite clearly by drawing tangents to the initial slope and the ending slope. The intersection of these two lines give the EYP. This is illustrated for PVC in Fig. 11a. As has been pointed out by Teoh *et al.* [3], one of the main advantages of stress partitioning is for the detailed definition of EYP which otherwise will be missed out in a conventional plot of applied stress and strain.

If the effective stress portion (see Fig. 1a) can be represented by a rate-activated dashpot filled with a non-Newtonian fluid following Eyring's hyperbolic relationship between strain rate and applied stress, then the viscous process can be treated as a thermally activated flow. Fig. 12a and b show that a linear relationship can be used to describe the relationship between the extrapolated yield stress (EYS) and  $\ln$  CHS for both PVC and PP. These relationships can be expressed, using linear regression analysis, as

$$\text{EYS (PVC)} = 10.31 + 2.131 \ln \text{CHS} \quad (12)$$

$$\text{EYS (PP)} = 4.66 + 1.335 \ln \text{CHS} \quad (13)$$

Eyring's equation can be written as

$$\sigma = C + \frac{2kT}{V} \ln \text{CHS} \quad (14)$$

where  $C$  is a constant,  $k$  is Boltzmann's constant,  $V$  is

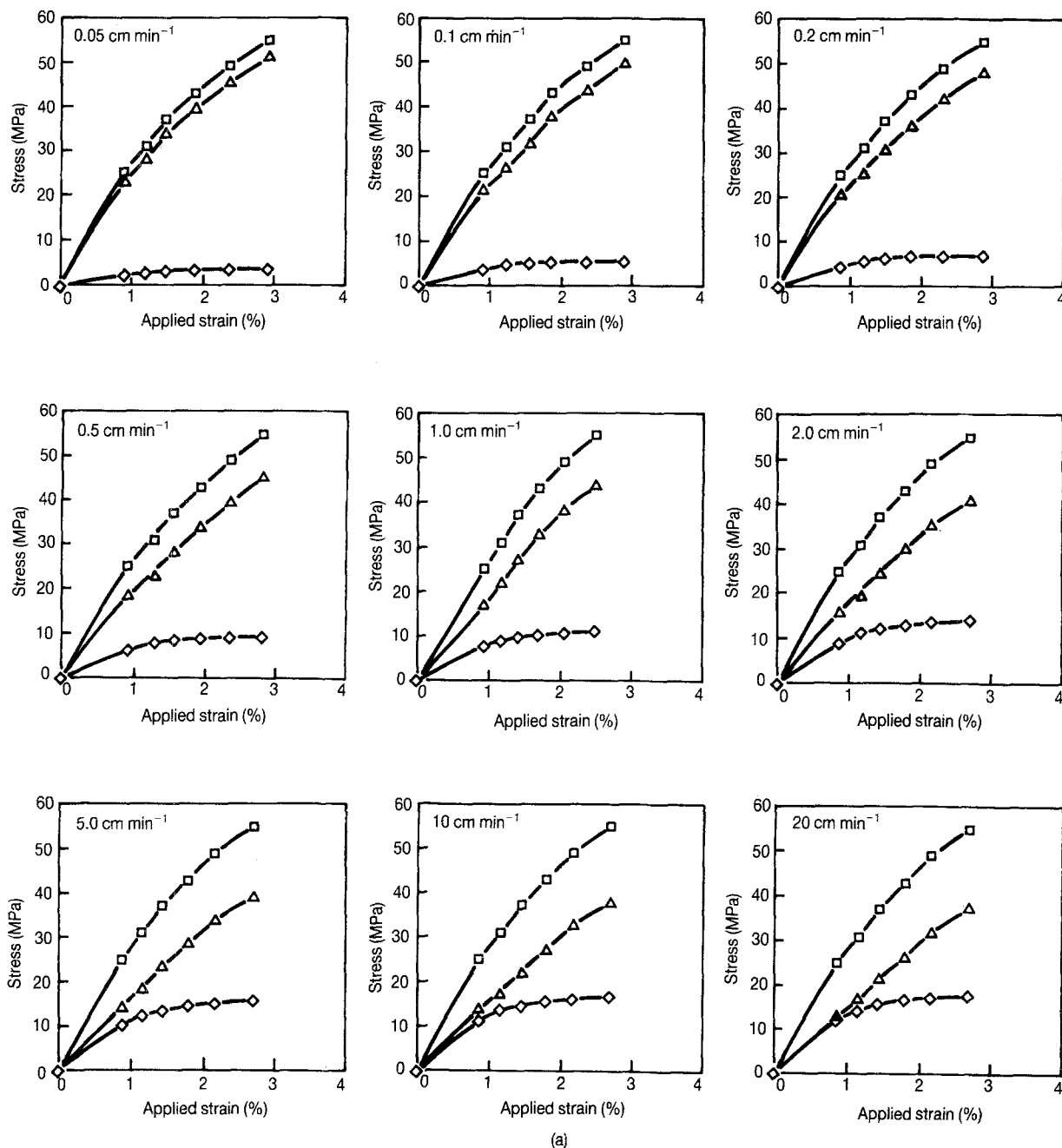
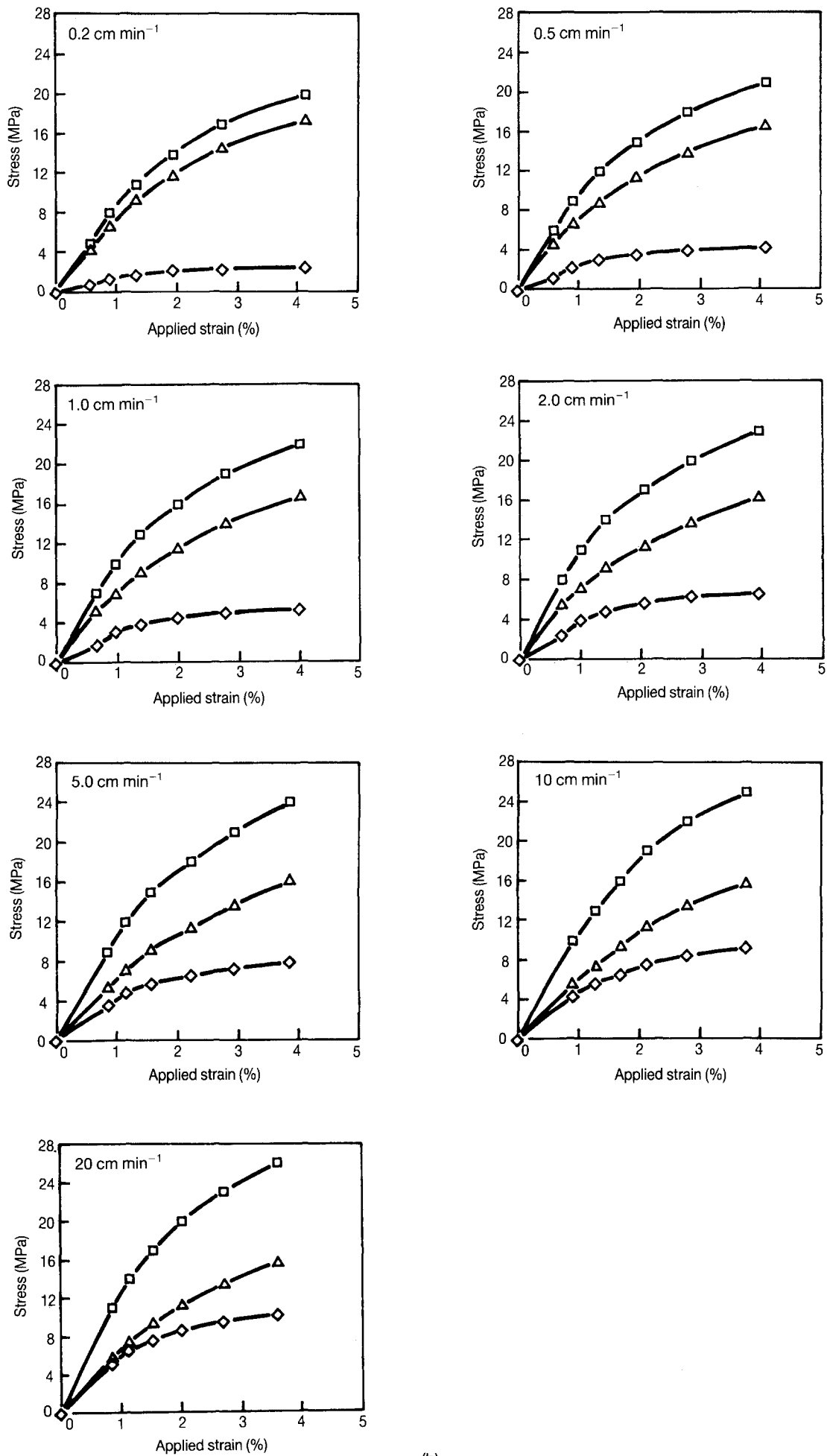


Figure 9 Variation of (□) applied, (△) recovery and (◇) effective stress with applied strain for (a) PVC and (b) PP.



(b)

Figure 9 (continued).

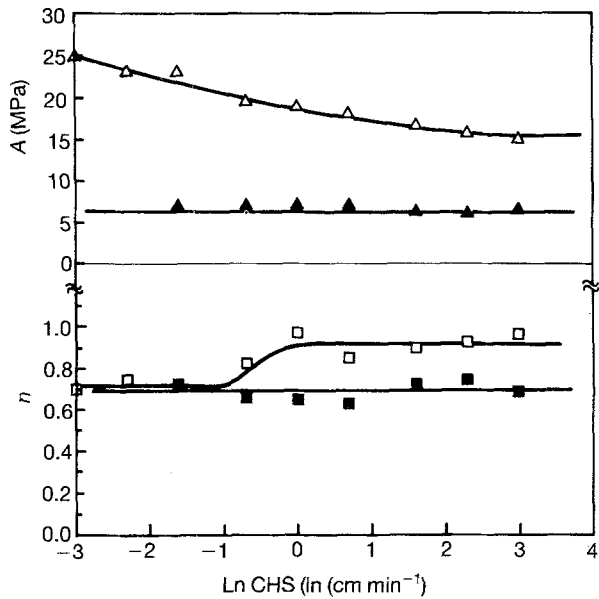


Figure 10 Variation of  $A$  and  $n$  with  $\ln$  CHS for ( $\square$ ,  $\triangle$ ) PVC and ( $\blacksquare$ ,  $\blacktriangle$ ) PP.

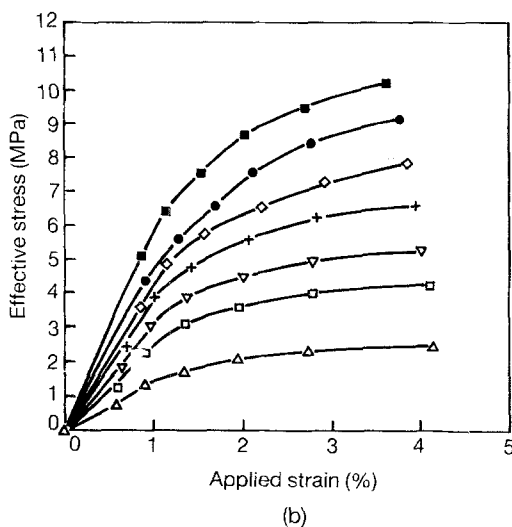
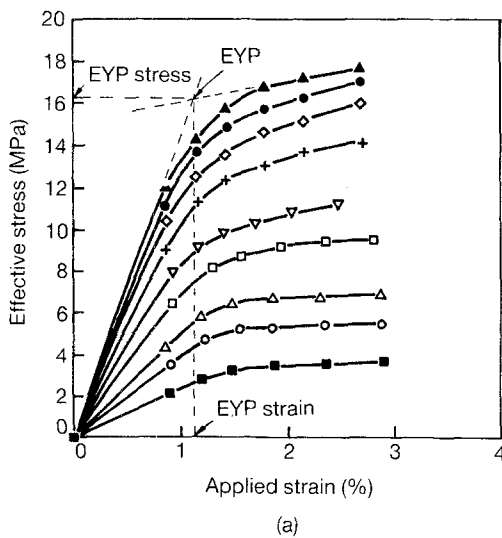


Figure 11 Variation of effective stress with applied strain for (a) PVC and (b) PP. CHS ( $\text{cm min}^{-1}$ ): ( $\blacksquare$ ) 0.05, ( $\circ$ ) 0.10, ( $\triangle$ ) 0.20, ( $\square$ ) 0.50, ( $\nabla$ ) 1.00, ( $+$ ) 2.00, ( $\diamond$ ) 5.00, ( $\bullet$ ) 10.00, ( $\blacktriangle$ ) 20.00.

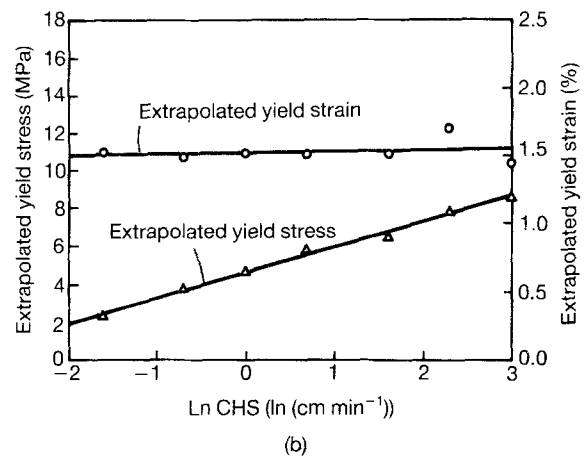
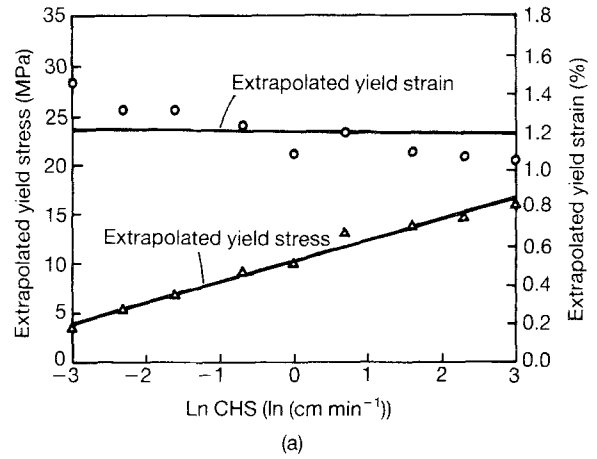


Figure 12 Extrapolated ( $\triangle$ ) yield stress and ( $\circ$ ) strain against  $\ln$  CHS for (a) PVC and (b) PP.

the activation volume and  $T$  is the absolute temperature. The gradient of EYS stress versus  $\ln$  CHS, therefore, could be used to calculate the activation volume. For PVC,  $V_{\text{PVC}} = 3.84 \text{ nm}^3$  and for PP,  $V_{\text{PP}} = 6.13 \text{ nm}^3$ . The significance of the activation volume has been well discussed by Kausch [12]. Nonetheless, it can be seen that the activation volume for PP is much larger than for PVC, indicating that the flow volume during plastic deformation is larger for ductile polymers such as PP than for less ductile polymers like PVC. If the activation volumes were calculated using Equations 6 and 7 instead, the values are  $V_{\text{PVC}} = 14.28 \text{ nm}^3$  and  $V_{\text{PP}} = 4.15 \text{ nm}^3$ . It can be noted that for a very ductile material (PP), the activation volume calculated from a plot of yield stress versus  $\ln$  CHS is comparable in magnitude whilst for a less ductile material (PVC), the activation volume calculated from a plot of yield stress versus  $\ln$  CHS can be extremely high (in this case, about four times larger).

From Fig. 12a and b, it can be seen that the strains at which yielding (as defined by EYP) occurs is much smaller (less than 2%) than those obtained from conventional stress-strain diagram (greater than 3% and 7% for PVC and PP, respectively). This observation indicates that plastic yielding occurs much earlier and values of yield strains obtained from conventional stress-strain diagrams are not accurate enough. This



finding also appears to support the work by Fotheringham and Cherry [4] who reported that plastic yielding occurs at a very early stage in the deformation of high-density polyethylene. For both PVC and PP, the extrapolated yield strain appears to average about 1.2% and 1.6%, respectively.

#### 4. Conclusion

Partitioning the applied stress into internal stress components is a useful approach towards a better understanding of the viscoelastic nature of polymers. In the work described here, the internal stresses of PVC and PP were measured successfully using the modified strain transient dip test on a computer-controlled electro-servo-hydraulic tensile testing machine built in the University. Useful results, such as yielding occurring at smaller strains, and the mathematical descriptions for the effective and recovery portions of stress allowed for a more detailed study of the deformation behaviour of PVC and PP. A power-law relationship can be used to describe the variation of the recovery stress with strain. When the power exponent,  $n$ , is greater than 0.67 cold-drawing did not occur before fracture. Actual values of yield strains obtained are smaller (less than 2%) than those obtained from conventional stress-strain diagrams (which for PVC and PP exceed 3.5% and 7%, respectively). This observation indicates that plastic yielding occurs much earlier and values of yield strains obtained from conventional stress-strain diagrams may be overestimates. It is noted that for a very ductile material (PP), the activation volume is comparable in magnitude to that obtained by the conventional method. For a less ductile material (PVC), the activation volume is about four times higher. One of the main advantages of stress partitioning is for the de-

tailed definition of the extrapolated yield point in the effective stress portion which otherwise will be missed out in a conventional plot of applied stress and strain.

#### Acknowledgement

The authors gratefully acknowledge a research grant (RP22/83) from the National University of Singapore.

#### References

1. S. H. TEOH, B. W. CHERRY and H. H. KAUSCH *Int. J. Damage Mech.* **1** (1992) 245.
2. S. H. TEOH, PhD thesis, Materials Engineering Department, Monash University, Australia (1992).
3. S. H. TEOH, C. L. CHUAH and A. N. POO, *J. Mater. Sci.* **22** (1987) 1397.
4. D. G. FOTHERINGHAM and B. W. CHERRY, *ibid.* **13** (1978) 951.
5. D. M. SHINOZAKI and C. M. SARGENT, *Mater. Sci. Eng.* **35** (1978) 213.
6. A. S. KRAUSZ and H. EYRING, "Deformation Kinetics" (Wiley, New York, 1975) p. 260.
7. C. N. AHLQUIST and W. D. NIX, *Scripta Metall.* **3** (1969) 679.
8. B. BERGMAN, *Scand. J. Metall.* **4** (1975) 109.
9. S. H. TEOH, A. N. POO, A. O. TAY and G. B. ONG, in "Proceedings of the International Conference on Plastics and Rubber Processing 1989—Automation and Computer", Singapore, edited by S. H. Teoh (Plastics and Rubber Institute, Singapore Section, 1989) p. 110.
10. A. O. TAY and S. H. TEOH, *Polym. Test.* **8** (1989) 231.
11. S. H. TEOH and B. W. CHERRY, *Polymer* **25** (1983) 727.
12. H. H. KAUSCH, "Polymer Fracture", 2nd Edn (Springer-Verlag, New York, 1987) p. 248.

*Received 26 October 1992  
and accepted 6 July 1993*